



Bayero Journal of Pure and Applied Sciences, 15(1): 95 - 104

Received: April, 2022

Accepted: May, 2022

ISSN 2006 – 6996

REMOVAL OF ERIOCHROME BLACK T DYE FROM AQUEOUS SOLUTION USING BASE ACTIVATED TYPHA GRASS (*Typha latifolia*) AS AN ADSORBENT

Ayuba, A. M. and Sani, M.*

Department of Pure and Industrial Chemistry, Faculty of Physical Sciences, College of Natural and Pharmaceutical Sciences, Bayero University, Kano, Nigeria

*e-mail address: musaniyaya@gmail.com

ABSTRACT

Adsorption of Eriochrome Black T (EBT) dye from aqueous solution by activated typha grass (*T. latifolia*) was studied using batch system. The adsorbent was characterized by Fourier transform infrared spectroscopy (FTIR), Scanning Electron Microscopy (SEM) methods, as well as the point of zero charge (PZC). Adsorption parameters including effect of contact time, adsorbent dose, initial dye concentration and pH were studied and the adsorption capacity (q_e) was found to be 47.619mg/g. The adsorption isotherm for the adsorption processes were also modelled and evaluated and the data fitted Freundlich isotherm model with R^2 of 0.9943 relative to other models tested. The kinetic data were best described by pseudo-second order model with R^2 values of 0.999 and rate constant (k) of $6.30\text{mol}^1\text{dm}^3\text{s}^{-1}$ out of the four models tested. The thermodynamic quantities of the adsorption process including the entropy change (ΔS) which describe the degree of disorderliness of the dye-adsorbent interphase was found to be $2.108\text{Jmol}^{-1}\text{K}^{-1}$ indicating an increase in the interphase disorderliness, the enthalpy change (ΔH) describing the nature of energetic interaction between the dye molecules and the adsorbent surface has a value of -9.223kJmol^{-1} proving an exothermic process and the Gibbs free energy change (ΔG) of the range -8.563 to -8.718kJmol^{-1} were obtained indicating the process to be feasible and spontaneous in nature. Hence, the activated carbon produced from typha grass can be a potential adsorbent for the removal of hazardous dyes such as Eriochrome Black T from industrial effluent.

Keywords: Adsorption, Kinetics, Thermodynamics, Equilibrium, Isotherms, Eriochrome Black T, *T. Latifolia*.

INTRODUCTION

The rate of our industrial development and its subsequent discharges to the environment has caused severe disturbing problems resulting in different levels of pollution. Water pollution in particular, is the major pollution source constituting industrial release comprising of dyes, heavy metals, pharmaceutical effluents, and several other organic contaminants. These pollutants are mostly non-biodegradable and responsible for genetic and physiologic problems in living organisms even at minute concentrations (Fu and Wang, 2011). However, in the last few years, dye wastewater has become a major challenge for clean water reservoirs due to its deleterious effects on water ecosystem. Dyes in wastewater are known to be responsible for unpleasant odour, carcinogenic and prevent sunlight transmission into fresh water, thus decreases photosynthesis and distorting the food chain in aquatic systems (Wang *et al.*, 2018).

Dye removal is an essential research subject to alleviate environmental pollution and its effects by reducing its impacts on ecosystems. There are many techniques which have been studied and applied to remove dyes from wastewater including physical, chemical and biological methods (Zarrini *et al.*, 2017).

Ion exchange, coagulation, biodegradation and precipitation are wastewater treatment techniques used to minimize dye molecules contamination. Some of these methods are known to offer advantages and limitations for dye removal from wastewater. The adsorption process is an effective technique to remove toxic pollutants including dye molecules from wastewater due to its ease of disposal, simple operation, cost effectiveness, high removal efficiency and flexibility in terms of the properties of adsorbent used as separation medium (Astuti *et al.*, 2019; Wang *et al.*, 2020).

Base activated typha grass was prepared in this research work primarily for the removal of Eriochrome Black T (EBT) dye which is a low-cost and environmentally friendly adsorbent (Zhang *et al.*, 2016). The adsorbent was selected to investigate its adsorption capacity for EBT dye present in aqueous solution, due to its availability, low cost and environmental consideration (Taufiq *et al.*, 2018). The effects of various parameters such as contact time, adsorbent dose, initial concentration, pH and temperature on the adsorption efficiency of EBT were studied using the batch technique. The kinetics of EBT adsorption onto activated typha

grass was evaluated by pseudo first order, pseudo second order, Elovich and Intraparticle diffusion kinetic models. Experimental equilibrium data were fitted to the Langmuir, Freundlich, Temkin and Dubinin Radushkevich isotherm equations to propose the mechanism for the adsorption process. This work is therefore aimed at establishing the potentials of a base treated typha grass as an adsorbent for the removal of EBT dye from synthetic wastewater through adsorptive, kinetic and thermodynamic parameters evaluation processes.

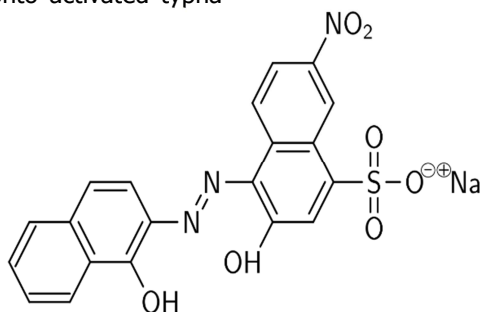


Figure 1. Chemical Structure of Eriochrome Black T

MATERIALS AND METHODS

Chemicals and Reagents

All chemical and reagents used in this study were obtained from Sigma-Aldrich Ltd., London which include Hydrochloric acid, Sodium hydroxide, while Eriochrome Black T Dye was obtained from Merck Chemicals. Ltd., Mumbai, India. All solutions were prepared using distilled water, and the chemicals were used without any further treatment.

EBT Dye Solution Preparation

The stock solution Eriochrome Black T was prepared by dissolving 1g of the dye into a 1L to produce 1000 mg/L using distilled water. The experimental solutions were later diluted to the required concentration for subsequent uses. The stock concentrations of 10 to 120 mg/L were prepared and used. Eriochrome Black T is toxic, non-biodegradable and water-soluble dye with following properties: molecular formula ($C_{20}H_{12}N_3O_7SNa$) and molecular weight (461.381g/mol) respectively. The concentration of the un-adsorbed EBT dye was measured at $\lambda_{max} = 524.44\text{nm}$ using UV-Visible Spectrometer (Perkin Elmer, Lambda 35).

Adsorbent Collection and Preparation

The typha grass was obtained from Marma town, Guri local government area of Jigawa State, Nigeria. The typha grass sample was initially washed with tap water then distilled water to remove the impurities (Nwosu *et al.*, 2017). The sample was air-dried then oven dried at 105°C . The dried sample was pulverized and

passed through a 2mm sieve. The sieved sample was activated with 0.5M NaOH in a ratio of 1:20 for 30 minutes as reported by Pandey *et al.* (2018).

Adsorbent Characterization

Activated typha grass was characterized by different modern techniques such as FT-IR and SEM. The FT-IR was employed for analysing the functional groups present and was scanned in the range of $650 - 4000\text{cm}^{-1}$ with a scan rate at 8cm^{-1} resolution. The investigation was carried out using Cary 630 Fourier Transform Infrared Spectrophotometer Agilent Technology. A scanning electron microscope (SEM) was employed to study the surface morphology surface of the adsorbent by a Phenom World Eindhoven microscope. An electron beam of energy of 20 kV was hired for the surface examination. Point of zero charge was also investigated to find pH at which the surface of the adsorbent is zero using salt addition method as reported by Bakatula (2018).

Adsorption studies

The activated typha grass (ATG) was employed for the adsorption of Eriochrome Black T (EBT) dye from aqueous solution. For establishing maximum adsorption capacity, the effect of various experimental factors such as contact time, temperature, adsorbent dose and initial dye concentration were studied and optimized. In a typical adsorption process, 0.02g of ATG was added to 20cm^3 of 50 mg/L dye solutions.

The solutions were then placed in a vacuum mechanical shaker with rpm 150 ± 4 for 60minutes at 298 K. After the time interval the dye solutions were centrifuged and then analyzed using UV-Vis spectrophotometer at 524.44nm for un-adsorbed EBT dye. The extent of adsorption of EBT dye by ATG adsorbent at various time intervals was calculated using equation 1 as reported by Ayuba and Idoko (2021).

$$\text{Adsorption Capacity } (q_e) = \frac{(C_0 - C_e) \times V}{m} \quad (1)$$

Where q_e is the adsorption capacity (mg/g), C_0 and C_e are the initial and final equilibrium concentration (mg/l) of EBT in solution, V is the volume of EBT solution (L), and m is the mass (g) of the adsorbent.

RESULTS AND DISCUSSION

The analysis of the functional groups present on the activated typha grass (ATG) before and after EBT dye adsorption was investigated using FTIR instrumental technique and the results are presented in Figure 2 and Table 1 respectively.

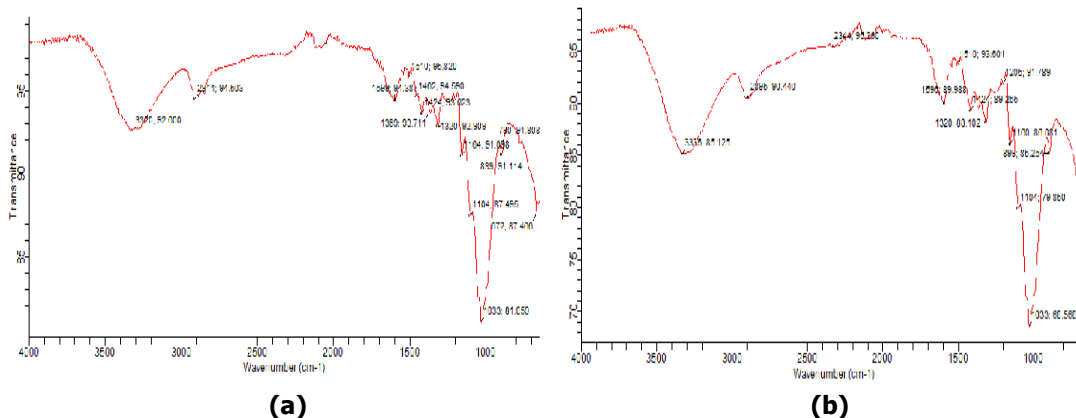


Figure 2. FTIR spectrum of ATG (a) before and (b) after adsorption of EBT dye

Table1: Different functional group recognized before and after adsorption of EBT onto ATG

Functional Group	Absorption range (cm ⁻¹)	Before absorption (cm ⁻¹)	After absorption onto EBT (cm ⁻¹)	Difference (cm ⁻¹)
OH stretch	3700-2500	3320	3335	15
C-H stretch	3000-2840	2914	2895	19
C=O stretch	1710-1580	1600	1612	12
C≡C stretch	1675-1550	1510	1510	0
C-O stretch	1080-1300	1104	1104	0

The FTIR spectrum of ATG with loaded EBT dye is shown in Fig. 2. The characteristic O-H, C-H, C=O, C≡C and C-O absorption bands were observed at 3320, 2914 1600, 1510 and 1104 cm⁻¹ in ATG before adsorption respectively (Chen *et al.*, 2005; Bajpai *et al.*, 2016). A broad band from 3700 to 2500 cm⁻¹ corresponds to the stretching vibration of hydroxyl group. The peak at 2895 cm⁻¹ mark the presence of C-H stretching group. Added, the peaks at 1612 cm⁻¹, 1510 cm⁻¹, and 1104 cm⁻¹ corresponds to the C=O stretching, bridge C≡C stretching, and C-O stretching, respectively (Arof *et al.*, 2010). Therefore, the presence of characteristic peaks of carbonyl and hydroxyl groups confirms the presence of desired functional units in the activated typha grass. The hydroxyl, carboxyl and carboxylic acid functional groups are vital

adsorption sites present in this adsorbent (Itodo *et al.*, 2011).

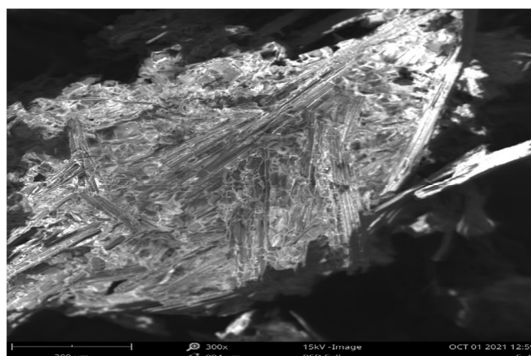
Scanning Electron Microscopy (SEM) was used to investigate the morphology of ATG and ATG loaded EBT. Fig. 3 shows the morphological changes of ATG. Blistered bunches and vague irregular porous shapes were formed. The smooth surface of the ATG after adsorption onto EBT became uneven permeable structures and various sized particles, thus increased the adsorption of EBT. The modification can be responsible for an increased surface area of ATG, but after adsorption the surface area has decreased (Dash *et al.*, 2016). Moreover, the structure and size of the ATG adsorbent loaded by EBT indicate considerable change. However, the surface is slightly rough, and organic matter like substances can be observed to stick to the particle surface, which was due to the growth of

adsorbed dyes on the surface of ATG. At the same time, it was found that the tendency of adhesion and aggregation between particles increases, which was due to the Van der Waals

force and hydrogen bond force between dye molecules adsorbed on different particle surfaces, resulting in the enhanced interaction between particles (Hussain *et al.*, 2022).



(a)



(b)

Figure 3. SEM Micrograph of ATG (a) before and (b) after adsorption of EBT. The points of zero charge PZC for ATG adsorbent is presented in Figure 4. At the PZC there is no surface charge to be neutralized by ions at the surface of ATG, and any adsorbed ions that exist must be bound in surface complexes. The PZC of ATG studied is as presented in figure 4 to be around 7, which indicate the presence of perfect charge balance

in the acidic medium the region among the equilibrated ions in an aqueous solution. Moreover, substrates with low PZC values show the highest tendency to treat effluents contaminated with cations, while substrates with high PZC values would be more appropriate to capture anions (Nasiruddin and Anila, 2007).

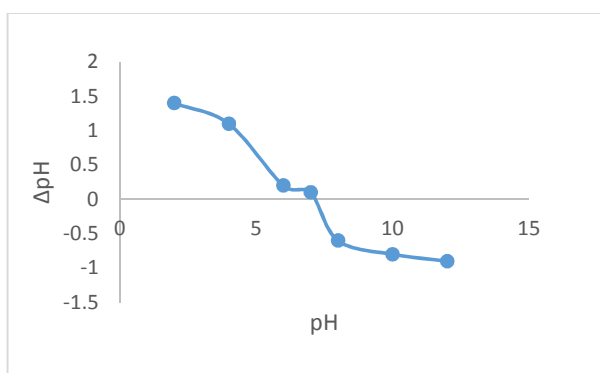


Figure 4. Point of zero charge of ATG

Optimization of Adsorption Parameters

The influence of contact time on the adsorption rate was studied. It was calculated at various time intervals between 5 and 120 min of contact between ATG and EBT molecules and the results are presented in Figure 5a. The adsorption of EBT was fast in the first 20- 60 minutes and dropped after 60 minutes, the rate became constant due to equilibrium attainment between the adsorbed EBT molecules to that remained in the solution (Hussain *et al.*, 2022). The initial fast phase may also be due to the increased number of vacant sites available at the initial stage whereas after 60 minutes, decreasing the

effect is due to vacant surface sites are not easy to be occupied due to repulsive forces. Therefore, further batch experiments were carried out at 60 minute optimal contact time (Ayuba and Thomas, 2020). The impact of using varying amounts of adsorbents dose (0.02–1.2g) was also evaluated and presented in Figure 5b. The decrease in adsorption per unit mass with increasing adsorbent dose is attributed to probable overlapping of adsorption sites as adsorbent dose increases which will equally reduce the effective adsorption sites. Similar trend was reported by Abdus-Salam and Adekola (2018).

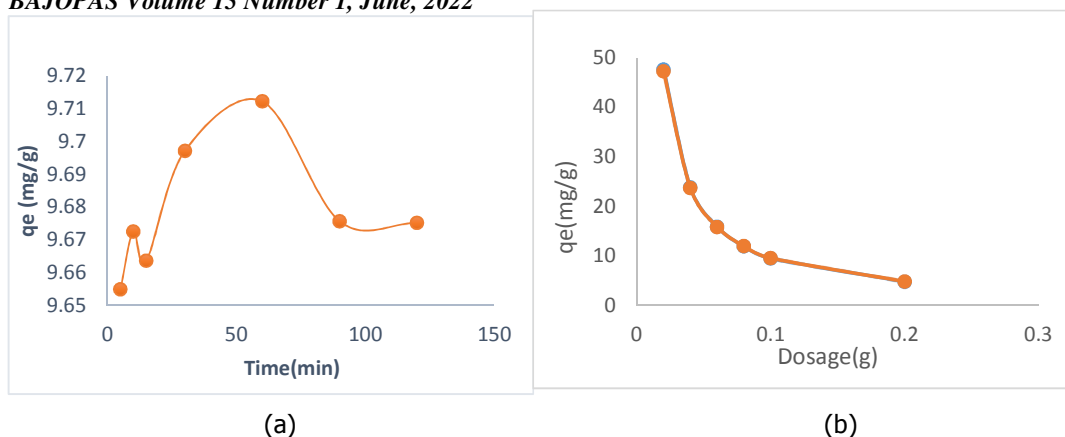


Figure 5. Effect of (a) contact time (b) adsorbent dose of the EBT adsorption onto ATG

Figure 6a and b shows the effect of initial concentration and solution pH on the adsorption of EBT dye onto ATG. However, the effect of EBT concentration was studied at three different temperatures, 298, 308, and 318 K. In addition, it was detected that the amount of EBT molecule adsorbed per gram of the ATG increased with increasing concentration of EBT at low concentration, the available driving force for transfer of EBT molecule onto the adsorbent particles is low, while at high concentration, there is a corresponding increase in the driving force, thereby enhancing the interaction between the EBT molecule in the aqueous phase and the active sites of the adsorbent (Nwosu *et al.*, 2017). Furthermore, the influence of pH on

EBT removal are calculated by changing initial pH of solution from 2 to 10. The solution pH is one of the key parameters that control the adsorption process. It controls the electrostatic interactions between the adsorbent and the adsorbate. As can be seen from Figure 6b the EBT removal was somewhat evidently dependent on pH with the better adsorption arising under neutral conditions (pH 7) and decreased with increase in solution pH. The higher adsorption was observed at pH 7 by ATG adsorbent. This means the adsorbed amount of EBT decrease as pH increased from 4 to 10 due to electrostatic repulsion between adsorbent and negatively charged species in solution (Ozacar, 2006; Vigneshwaram *et al.*, 2021).

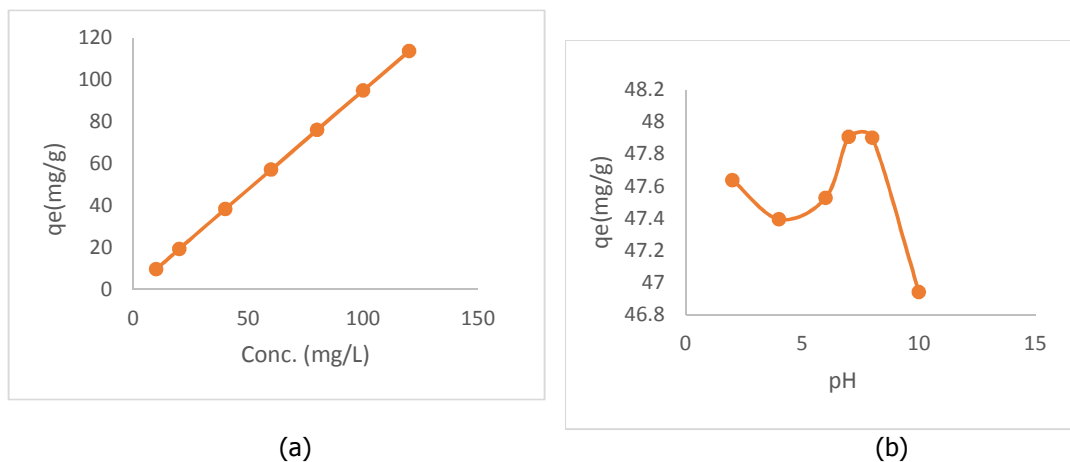


Figure 6. Effect of (a) initial concentration (b) pH of EBT adsorption onto ATG

Isotherms Studies

Isotherm studies are quite essential in understanding the mechanism of undertaken adsorption data (Kamau and Kamau, 2017). In this current study, four adsorption isotherms; Langmuir, Freundlich, Temkin and D-R models were applied and evaluated at three different temperatures 298, 308, and 318 K with varying

concentrations between 10 and 120 ppm. Results of the analysed isotherm data were evaluated and the applicability of each model was ascertained by relatively comparing the correlation coefficient (R^2) of their linear fit. Linear equations of the four models are presented in equations (3 - 6) respectively (Dada *et al.*, 2012):

$$\frac{1}{q_e} = \frac{1}{Q_o} + \frac{1}{Q_o K_L C_e} \quad \text{Langmuir} \quad (3)$$

$$\log Q_e = \log K_f + \frac{1}{n} \log C_e \quad \text{Freundlich} \quad (4)$$

$$q_e = B_T \ln C_e + B_T \ln K_T \quad \text{Temkin} \quad (5)$$

$$\ln q_e = \ln q_m - \beta \varepsilon^2 \quad \text{Dubinin Radushkevich (D-R)} \quad (6)$$

Where C_e represents the equilibrium dye concentration (mg/L); q_e and Q_o represents the equilibrium and maximum adsorption capacity (mg/g); K_L , K_f , K_T and β denotes the Langmuir, Freundlich, Temkin and D-R constants, respectively, while n denotes the adsorption intensity. Comparison of the linear fit of the four isotherm models showed that Freundlich isotherm model with $R^2 = 0.9943$ relatively show a better fit when compared to others. This shows that Freundlich isotherms best explaining the adsorption process mechanism as compared to Langmuir, Temkin and D- R models (Zhou *et al.*, 2018). Based on the underlying principles of Freundlich isotherm which this process is obeying, it can be demonstrated that the adsorption of EBT dye onto the studied adsorbent is controlled by physical adsorption process and the surface of the adsorbent is characterized with heterogeneous adsorption

sites. Values of isotherm constants and parameters are presented in table 2 and Figure 7 respectively.

However, from Table 2 the value of rate constant, K_L identifies the extent of interactions between the adsorbent surface and adsorbate molecules. In the case of the Freundlich model, the value of $1/n$ obtained is below 1 indicating the favourable adsorption condition (Ahmed *et al.*, 2021).

Kinetic Studies

The kinetic models tested for this studies to determine the adsorption rate of EBT dye from aqueous solution onto ATG. In particular, an EBT solution of 50 mg/L was prepared and mixed with 0.02g adsorbent. Samples were taken out at various time intervals between 10 and 120 min.

Table 2. Adsorption Isotherm constants for the adsorption of EBT onto ATG

Parameter	Eriochrome Black T
	Langmuir
Q_o (mg/g)	1250
K_L (L/mg)	0.017316
R_L	0.535962
R^2	0.9404
	Freundlich
$1/n$	0.9077
N	1.101686
K_F	0.890012
R^2	0.9943
	Temkin
A_T	0.54442
B_T	67.0430
B	37.575
R^2	0.9268
	Dubinin-Radushkevich
q_m (mg/g)	79.814
K_{dr} (mol ² /KJ ²)	3.0×10^{-7}
E (KJ/mol)	0.129
R^2	0.8994

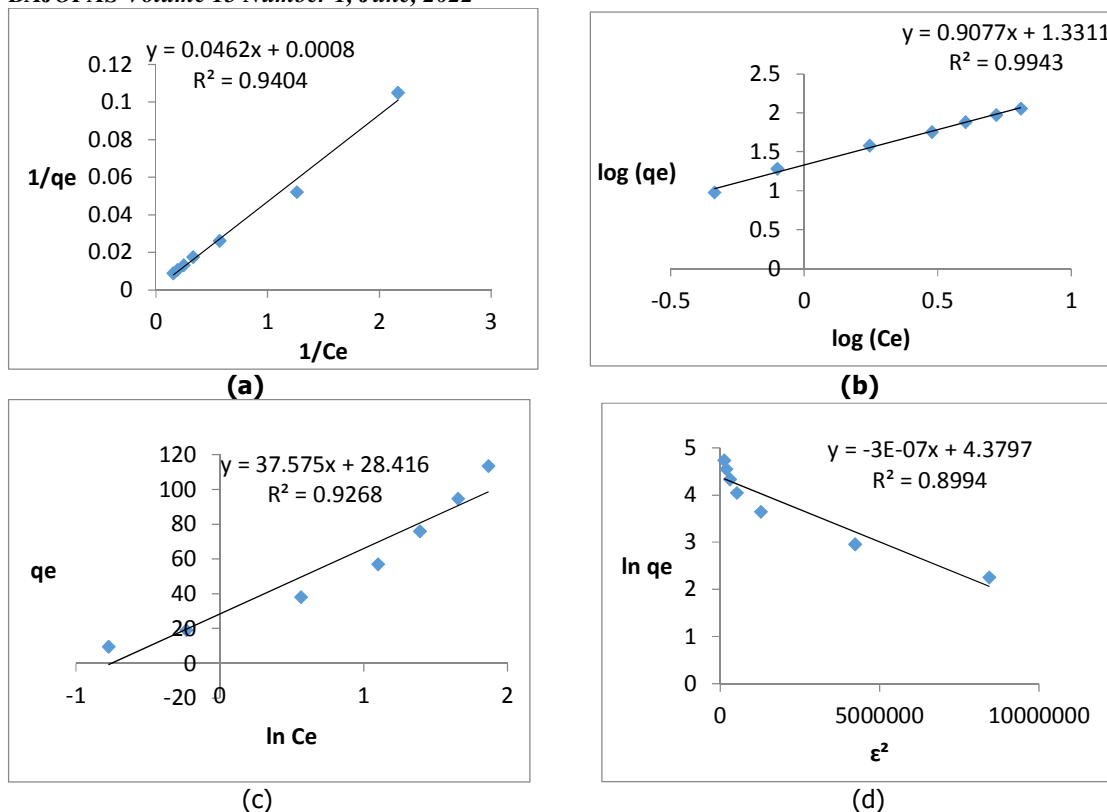


Figure 7. Adsorption Isotherms of (a) Langmuir (b) Freundlich (c) Temkin (d) D-R of ATG-loaded EBT.

Four kinetics models; pseudo-first order and pseudo-second order, Elovich and Intraparticle diffusion were used for the evaluation of kinetic

data. Equations representing the mentioned models are presented as reported by Ayuba *et al.* (2020).

$$\log(q_e - q_t) = \log(q_e) - \frac{K_1}{2.303} t \quad (\text{Pseudo - First order}) \quad (7)$$

$$\frac{t}{q_t} = \frac{1}{K_2 q_e^2} + \frac{1}{q_e} t \quad (\text{Pseudo - Second order}) \quad (8)$$

$$q_t = \frac{1}{\beta} \ln(\alpha\beta) + \left(\frac{1}{\beta}\right) \ln t \quad (\text{Elovich}) \quad (9)$$

$$q_t = C + K_{int} t^{1/2} \quad (\text{Intraparticle Diffusion}) \quad (10)$$

Where K_1 , K_2 and K_{int} represents the pseudo-first order, pseudo-second order, Elovich and Intraparticle diffusion rate constant, q_e and q_t represents the adsorption amount at equilibrium and at time t (mg/g).

Figure 8 presents the kinetic results undertaken for the study of adsorption of EBT onto ATG and the values of rate constants and q_e as obtained from pseudo-first and pseudo-second order, Elovich and Intraparticle diffusion are presented in Table 3.

Table 3. Kinetic parameters for the adsorption of EBT onto ATG

Kinetic Models	Parameters			
Pseudo-first order	$q_{e,Cal}(mg/g)$ 47.799	$q_{e,Exp}(mg/g)$ 0.175	$k_1(\text{min}^{-1})$ 0.0057	R^2 0.023
Pseudo-second order	$q_{e,Cal}(mg/g)$ 47.789	$q_{e,Exp}(mg/g)$ 47.619	$k_2(\text{mol dm}^{-3} \text{min}^{-1})$ 6.30	R^2 0.999
Elovich		B 38.759	A 5.23×10^{19}	R^2 0.200
Intraparticle Diffusion		k_3 -0.012	C 12.140	R^2 0.126

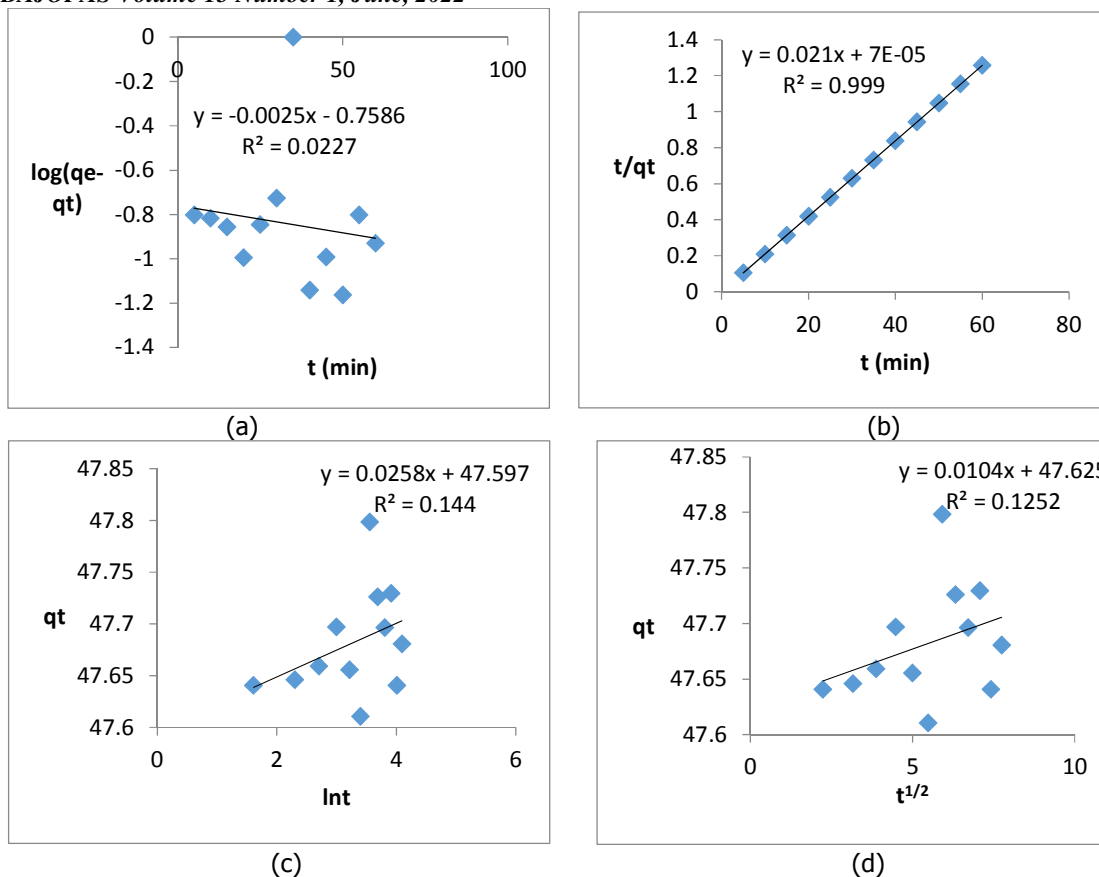


Figure 8. Adsorption Kinetics of (a) first order (b) second order (c) Elovich (d) Intraparticle diffusion of EBT-loaded ATG

However, based on assessment of correlation coefficient values of the four models, the pseudo-second order was found to be relatively favoured compared to other models tested, which suggest the involvement of chemical interactions in the EBT adsorption. In addition, $q_{e,cal}$ values as determined from the pseudo-second order are found to be comparable to $q_{e,exp}$ that also simplifies its fitness in comparison to pseudo- second order (Li *et al.*, 2019; Yao *et al.*, 2020).

Thermodynamics study

To further establish the mechanism of the adsorption process, thermodynamic studies were carried out to investigate the influence of

temperature on ATG adsorption of EBT from the synthetic wastewater by varying the operational temperature from 30°C to 50°C (303 - 323K). Gibb’s free energy (ΔG), enthalpy (ΔH) and entropy (ΔS) changes of the adsorption process were determined using the following equations:

$$\Delta G = -RT \ln K_L \tag{11}$$

$$\ln K_L = \frac{\Delta H}{RT} + \frac{\Delta S}{R} \tag{12}$$

ΔG was determined using Equation (11), while ΔH and ΔS were determined from Equation (12) by the linear plot of $\ln K_L$ versus $1/T$ (K), ΔH was evaluated from the slope and ΔS from the intercept of the plot.

Table 4. Thermodynamic parameters for the adsorption of ATG-loaded EBT

T (K)	K_L	ΔG (kJ/mol)	ΔH (kJ/mol)	ΔS (J/mol.K)
303	29.941	-8.563	-9.223	2.108
313	27.340	-8.609		
323	23.855	-8.718		

The values of ΔG , ΔH and ΔS for the adsorption of EBT onto ATG at three different temperatures are presented in Table 4. The negative values of ΔG shows the feasibility and spontaneous nature of the process, which is also indicative of the

physical nature of the adsorption process. This is because the values are less than the threshold value of -20kJ/mol for chemical adsorption (Sharma *et al.*, 2021).

Furthermore, the negative value of ΔG increased with temperature increase from 303 to 323 K indicating the adsorption is improved at higher temperature. However, the negative value of ΔH obtained for the adsorption process which describes the energetics involved at the interphase of the interaction between the dye

molecule and the adsorbent surface indicates the exothermic nature of the process (Adeyinka, 2019). Increase in positive value of entropy change shows that the adsorption process is characterized by an increase in degree of randomness at the dye-adsorbent surface qualifying a spontaneous process.

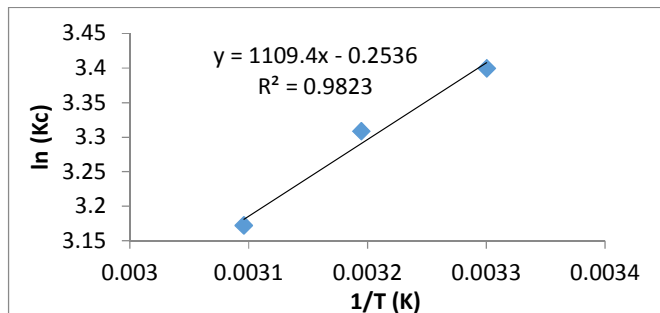


Figure 9. Van't Hoff plot for EBT adsorption at different temperatures

CONCLUSION

The results of this study showed that the base activated typha grass (ATG) is a potential adsorbent for the removal of Eriochrome Black T (EBT) dye from aqueous solution. The adsorbent prepared to study the effect of contact time, adsorbent dose, initial concentration, temperature and pH which are dependent on the efficiency of adsorption. The obtained adsorption kinetics fitted well with pseudo-second order

model, and the adsorption isotherms was best described by the Freundlich isotherm model for EBT. The adsorption thermodynamics process was feasible and spontaneous. However, the results projected that ATG had the potential to become a promising adsorbent for removal of EBT-contaminated wastewater. Additionally, ATG can also be an interesting alternative to stem out the impending water pollution caused by dyes in real life applications.

REFERENCES

- Abdus-Salam, N. Adekola, S. K. (2018). Biosorption of Dyes, *Applied. Water Science* 28-222 <https://doi.org/10.1007/s13201-018-0867-7>.
- Adeyinka S. Y. (2019). Adsorption of hexavalent chromium from aqueous solution by *Leucaena leucocephala* seed pod activated carbon: equilibrium, kinetic and thermodynamic studies, *Arab Journal of Basic and Applied Sciences*. 2576-5299 <https://doi.org/10.1080/25765299.2019.1567656>
- Ahmed, A., Ali, A., Ahmed, M., Parida, K.N., Ahmad, A.J.S. Ahmad, P. (2021). Technology, Construction and topological studies of a three dimensional (3D) coordination polymer showing selective adsorption of aromatic hazardous dyes, 265, 118482.
- Arof, A., Shuhaimi, N., Alias, N., Kufian, M., Majid, S., (2010). Application of chitosan/ iota-carrageenan polymer electrolytes in electrical double layer capacitor (EDLC). *Journal of Solid State Electrochemistry*. 14, 2145–2152.
- Astuti, W., Chafidz, A., Wahyuni, E.T., Prasetya, A., Bendiyasa, I.M., Abasaeed, A.E., (2019). Methyl violet dye removal using coal fly ash (CFA) as a dual sites adsorbent. *Journal of Environmental Chemical Engineering*. 7, 103262 <https://doi.org/10.1016/j.jece.2019.103262>.
- Ayuba, A. M. and Idoko, B. (2021). Cowpea husk adsorbent for the removal of crystal violet dye from aqueous solution, *Arabian Journal of Chemical and Environmental Research* 08(01): 114–132.
- Ayuba, A. M. Ladan, M. Muhammad, A. S. (2020). Thermodynamic and kinetic study of Pb (II) amputation by river sediment. *Applied Journal of Environmental Engineering Science* 6(3): 213-226.
- Ayuba, A. M. Thomas, A. N. (2020). Kinetic and equilibrium studies of paraquat dichloride adsorption on raw Bambara groundnut (*vigna subteranean*) shells *Applied Journal of Environmental Engineering Science* 6 (1) 1-13.
- Bajpai, M., Bajpai, S., Jyotishi, P., (2016). Water absorption and moisture permeation properties of chitosan/poly (acrylamide-co-itaconic acid) IPC films. *International Journal Biological Macromolecules*. 84, 1–9.
- Bakatula, E. N. Richard, Dominique, Neculita, Carmen Mihaela Zagury, Gerald J. (2018) Determination of point of zero charge of natural organic materials *Environmental Science and Pollution Research*.
- Chen, K. S., Ku, Y. A., Lin, H. R., Yan, T. R., Sheu, D. C., Chen, T. M., Lin, F. H., (2005). Preparation and characterization of pH sensitive poly (N-vinyl-2-pyrrolidone/ itaconic acid) copolymer hydrogels. *Material*

- Chemistry and Physics Journal*. 91, 484–489.
- Dada, A., Olalekan, A., Olatunya, A., Dada, O., (2012). Langmuir, freundlich, temkin and dubinin–radushkevich isotherms studies of equilibrium sorption of Zn^{2+} unto phosphoric acid modified rice husk. *IOSR Journal of Applied Chemistry*. 3, 38–45.
- Dash, S., Chaudhuri, H., Udayabhanu, G., Sarkar, A., (2016). Fabrication of inexpensive polyethylenimine-functionalized fly ash for highly enhanced adsorption of both cationic and anionic toxic dyes from water. *Energy & Fuels Journal* 30 (8), 6646–6653. <https://doi.org/10.1021/acs.energyfuels.6b00900>.
- Fu, F., Wang, Q., (2011). Removal of Heavy Metal Ions from Wastewaters: a review. *Journal of Environmental Management*. 92, 407–418.
- Hussain, Z. Chang, N. Sun, J. Xiang, S. Ayaz, T. Zhang, H. Wang, H. (2022). Modification of coal fly ash and its use as low-cost adsorbent for the removal of directive, acid and reactive dyes *Journal of Hazardous Materials* 4(22) 126-778.
- Itodo, U., Usman A. and Ugboaja, C. (2011). A Rate Study of Received and Derived Activated Carbon and Pseudo Constants for Methyl Red Sorption. *Journal of Encapsulation and Adsorption Sciences*, 1:57- 64.
- Kamau, J., Kamau, G., (2017). Modeling of experimental adsorption isotherm data for chlorothalonil by nairobi river sediment. *Modern Chemistry and Applications* 5, 2.
- Li, Changsheng. Zhang, Nan Chen, Jixiao. Ji, Jiawen Xue, Liu, Wang, Jianli Zhu, Jianhui and Ma, Yongqiang (2019) Temperature and pH sensitive composite for rapid and effective removal of sulfonyleurea herbicides in aqueous solution *Journal of Environmental Pollution* 255 113150 <https://doi.org/10.1016/j.envpol.2019.113150>.
- Nasiruddin Khan, M., Anila, S. (2007) Determination of points of zero charge of natural and treated adsorbents. *Surface Review and Letters*, Vol. 14, No. 3 (2007) 461–469.
- Nwosu, F.O., Adekola, F.A., Salami, A.O., (2017). Adsorption of N-nitrophenol (PNP) Using Pilli nut shell action. *Pak. J. Anal. Environ. Chem.* 18 (1), 69. <https://doi.org/10.21743/pjaec/2017.06.07>.
- Ozacar, M. (2006) Treatment of dairy wastewaters by electrocoagulation using mild steel electrodes. *Journal of Hazardous Materials*. 137 218–225.
- Pandey, R. Prasad, R. L., Ansari, N. G. and Chavali, M. (2018) Utilization of NaOH modified *Desmostachya bipinnata* (Kush grass) leaves and *Bambusa arundinacea* (bamboo) leaves for Cd (II) removal from aqueous solution, *Journal of Environmental Chemistry Engineering*. 3 (1) 593–602.
- Sharma, G., Kumar, A., Naushad, M., Thakur, B., Vo, D.V.N., Gao, B., Al-Kahtani, A.A., Stadler, F.J., (2021). Adsorptional-photocatalytic removal of fast sulphon black dye by using chitin-cl-poly (itaconic acid-co-acrylamide)/zirconium tungstate nanocomposite hydrogel. *Journal of Hazardous Material*. 416, 125714.
- Taufiq, A., Hidayat, P., Hidayat, A., (2018). Modified coal fly ash as low cost adsorbent for removal reactive dyes from batik industry. MATEC Web Conferences. 154, 01037. <https://doi.org/10.1051/mateconf/201815401037>.
- Vigneshwaran, S., Sirajudheen, P., Karthikeyan, P., Meenakshi, S., (2021). Fabrication of sulfur-doped biochar derived from tapioca peel waste with superior adsorption performance for the removal of Malachite green and Rhodamine B dyes. *Journal Surfaces and Interfaces* 23, 100920.
- Wang, X., Jiang, C., Hou, B., Wang, Y., Hao, C., Wu, J., (2018). Carbon composite lignin-based adsorbents for the adsorption of dyes. *Journals Chemosphere* 206, 587–596. <https://doi.org/10.1016/j.chemosphere.04.183>.
- Wang, H. Li, Z. Yahyaoui, S. Hanafy, H. Seliem, M. K. Bonilla-Petriciolet, A. Dotto, G. L. Sellaoui, L. Li, Q (2020) Effective adsorption of dyes on an activated carbon prepared from carboxymethyl cellulose: Experiments, characterization and advanced modelling. *Journal of Chemical Engineering*. S1385-8947(20)34232-7 <https://doi.org/10.1016/j.cej.2020.128116>
- Yao, X., Ji, L., Guo, J., Ge, S., Lu, W., Chen, Y., Cai, L., Wang, Y., Song, W., (2020). An abundant porous biochar material derived from wakame (*Undaria pinnatifida*) with high adsorption performance for three organic dyes. *Bioresources Technology Journal*. 3(18), 124082.
- Zarrini, K., Rahimi, A.A., Alihosseini, F., Fashandi, H., (2017). Highly Efficient Dye Adsorbent Based on Polyaniline-coated Nylon-6 Nanofibers. *Elsevier Ltd*, p. 142.
- Zhang, M., Mao, Y., Wang, W., Yang, S., Song, Z., Zhao, X., (2016). Coal fly ash/CoFe₂O₄ composites: a magnetic adsorbent for the removal of malachite green from aqueous solution. *Journal of Hazardous Materials* 6 (96), 93564–93574. <https://doi.org/10.1039/c6ra08939a>.
- Zhou, Y., Hu, Y., Huang, W., Cheng, G., Cui, C., Lu, J., (2018). A novel amphoteric cyclodextrin-based adsorbent for simultaneous removal of cationic/anionic dyes and bisphenol A. *Chemical Engineering Journal* 341, 47–57. <https://doi.org/10.1016/j.cej.2018.01.155>.